GSA Data Repository 2015307

Focused fluid transfer through the mantle above subduction zones (supplementary information)

Cassian Pirard[1,2] and Joerg Hermann[1]

[1]Research School of Earth Sciences, The Australian National University, Mills Rd. Building 61, ACT0200, Canberra, Australia

[2]Earth & Oceans, James Cook University, James Cook Drive, Building 34, QLD 4811, Townsville, Australia

STARTING MATERIALS & EXPERIMENTAL PROCEDURE

The starting material in the experiments is composed of an ultramafic and a felsic component. The ultramafic component was made of inclusion-free San Carlos olivine (Table DR3) crushed into two separate fractions. For mixed experiments (to constrain porous flow) we used a fine-grained powder (<5 µm grain size) to maximise interaction between ultramafic and felsic components. For experiments mimicking veins produced by focussed flow, we used a much larger grain size (80-100 µm) to enhance potential fluid migration perpendicular to the contact between ultramafic and felsic material. The felsic component was prepared from tetraethoxysilane mixed with various concentrations of trace elements added as nitrates (doped at low levels of a few tens of ppm) and transformed into a xerogel. This silica gel was milled and mixed with various amount of $Al(OH)_3$, fayalite, MgO and TiO_2 and a series of decarbonated and dehydrated compounds ($MnCO_3$, $CaCO_3$, K_2CO_3 and Na_2CO_3). Additional water was introduced with a micro-syringe in cold-seal silver capsules (Hack and Mavrogenes, 2006) where felsic glasses are synthesised at 800 °C and 1.5 GPa for 48 h. The compositions of starting sediment melts were analysed for major element composition using a raster beam in a SEM equipped with EDS and trace element composition using Laser Ablation ICP-MS (Table DR5).

100 mg of starting material (75 % of fine-grained olivine mixed 25 % of felsic glass) was loaded into 3.5 mm diameter gold capsules for the mixed experiments. Layered experiments had a bottom layer of ~50 mg of coarse olivine and a top layer of ~50 mg of finely crushed felsic glass (Figure 1). All experiments also contained a bottom layer of 10 mg of vitreous carbon spheres (ø = 120 to 150 µm) acting as fluid traps (Schwab and Johnston, 2001). The oxygen fugacity in the experiments is not buffered but the presence of water and carbon constrains the oxygen fugacity in these types of experiments to range between QFM-1 to QFM-3 (Pirard and Hermann, 2015). The fully loaded capsule (~7 mm in length) was wrapped in wet tissue to prevent excessive heating and evaporative water loss during arc welding and the weight was checked before and after welding to confirm water retention. Experiments were performed at 3.5 GPa and temperatures from 800 to 1100 °C using a 200 tonne, end-loaded 1.27 cm piston-cylinder apparatus housed at the Research School of Earth Sciences, ANU. Gold capsules were positioned in the hot spot of a 300 mm long, low-friction dry furnace assembly consisting of Teflon foil, salt outer sleeve, graphite heaters and MgO inserts. Temperature was controlled using a Eurotherm 904 device connected to a type-B thermocouple ($Pt_{94}Rh_6/Pt_{70}Rh_{30}$) protected by mullite ($Al_{(4+2x)}Si_{(2-2x)}O_{(10-x)}$) tubing. Pressure is converted directly from load and was controlled manually.

Experiments were initiated at room temperature and ~0.7 GPa to prevent water leakage. Pressure-temperature conditions were set along 2.5 °C/s – 8 MPa/s

gradients. After reaching set P-T conditions, runs were held for a week with pressure adjusted manually during the first 24 h to compensate for the release of internal friction. Temperature was automatically controlled and is accurate to ±10 °C with a precision of ±2 °C for the duration of the experiment.

Runs were quenched to <100 °C in under 10 seconds. The recovered gold capsules were grinded down to expose the sample and impregnated with epoxy resin to ensure cementation of the carbon spheres and limit any desegregation during the polishing process in kerosene (Fig. DR3).

ANALYTICAL METHODS

We examined the run products (phase assemblage) with reflected light microscopy and SEM. Mineral compositions were determined using a JEOL 6400 SEM (Electron Microscopy Unit, ANU) with an EDS system calibrated on known mineral standards produced by Astimex Scientific, operating at 15 kV with a focussed beam of 1 nA and a counting time of 120 s. Average analyses are based on an average of 6 spot analyses. Volatile-rich glasses, quenched materials and complex mixtures of hydrous phases were analysed using raster analyses.

Major and trace elements of minerals, glasses and quench material were analysed by laser ablation inductively coupled plasma mass spectrometry (LA-ICP-MS) at RSES, ANU using a pulsed 193 nm ArF Excimer laser with 3-7 mJ of output energy and a repetition rate of 5 Hz (Eggins et al., 1998), coupled to an Agilent HP7500 quadrupole ICP-MS system. Laser sampling was performed in an Ar atmosphere with He-H_2 (ratio 15:1) as a carrier gas. We applied various spot sizes (30 to 250 µm) and used multiple grains (more than 3) and fluid traps (more than 6 spots) to evaluate homogeneity. ^{29}Si was used as internal standard for minerals and glasses and NIST SRM 612 glass as external standard with reference values (Pearce et al., 1997; Keller et al., 2008). BCR-2G glass was used as a secondary standard and reproducibility was generally better than 9 % and accuracy better than 7 %.

DETERMINATION OF HYDROUS MELTS AND AQUEOUS FLUID COMPOSITIONS

Hydrous melt compositions were determined on the basis of a combination of SEM analyses of melt ponds occurring interstitially between minerals and laser ablation and SEM analyses of quenched material in the fluid traps and melt ponds (Table DR5).

Quench products from aqueous fluids are scarce and only rarely shards of glass can be analysed with SEM-EDS. Instead major and trace element analysis of quenched aqueous fluids was done by laser ablation of fluid traps. This technique provides major and trace element ratios of the quench material. These element ratios are converted into absolute composition using mass balance calculations for highly incompatible elements. In previous experiments, Cs has been used for quantification of fluid compositions using this approach (Tenthorey and Hermann, 2004; Kessel et al., 2004), but the significant amount of Cs in phlogopite made this approach fail. The analyses of all phases in the run products revealed that La, Ce, Nb, Ta, U and Th are highly incompatible in ultramafic solid phases (Fig. 3) and thus can be used as internal standards to quantify the fluid composition. The concentration of these

elements in the fluid phase was determined using an iterative approach. An initial modal proportion of solid phases and fluids was estimated based on SEM imaging of the charges. Then a mass balance was performed to evaluate the amount of H_2O stored in hydrous phases. The residual amount of water was combined with the incompatible elements to derive H_2O/(Nb, Ta, U, Th) of the fluids. The major element composition of the fluid was then obtained from the measured ratio of the major elements with respect to Nb, Ta, U and Th and the additional constrain that all solutes + H_2O must total 100 %. This calculated fluid composition was then inserted into mass balance calculations to further refine the estimation of modal proportions of minerals and fluid phases. Through a cycle of two iterations, fluid and modal compositions become robust and converge to stable values (Table DR6) (Pirard and Hermann, 2015).

Analyses of quenched aqueous fluids often represent a mixture of precipitates and amphibole, which is the most commonly observed mineral formed by dissolution-precipitation reaction in the fluid traps during the experimental run. Based on the MgO content found in aqueous fluids in equilibrium with peridotites (Stalder et al., 2001; Mibe et al., 2002; Dvir et al., 2010) and SEM observations, it appears that amphibole contributes to around 10 % of ablated material from quenched fluid analyses (Pirard and Hermann, 2015). In Table DR6, we provide initial calculated fluid composition through mass balance and the effect of amphibole subtraction (if any) on fluid composition. In Figure 3 and 4, aqueous fluid data is given for Nb normalisation and for 10 % subtraction of amphibole contaminant.

SUPPLEMENTARY REFERENCES

Dvir, O., Pettke, T., Fumagalli, P. & Kessel, R., 2010, Fluids in the peridotite-water system up to 6 GPa and 800ºC: new experimental constrains on dehydration reactions. Contributions to Mineralogy and Petrology, v. 161, p. 829-844.

Eggins, S.M., Kinsley, L.P.J. & Shelley, J.M.G., 1998, Deposition and element fractionation processes during atmospheric pressure laser sampling for analysis by ICP-MS. Applied Surface Science, v. 129, p. 278-286.

Hack, A.C. & Mavrogenes, J., 2006, A cold-sealing capsule design for synthesis of fluid inclusions and other hydrothermal experiments in a piston cylinder apparatus. American Mineralogist, v. 91, p. 203-210.

Jenner, F.E. & O'Neill, H.St.C. 2012, Analysis of 60 elements in 616 ocean floor basaltic glasses. Geochemistry Geophysics Geosystems, v. 13, Q02005, http://dx.doi.org/10.1029/2011GC004009.

Kelemen, P.B., Kikawa, E., Miller, D.J. et al., 2004, Leg 209. Proc. Ocean Dril. Prog., Initial Reports, v. 209

Keller, N., Arculus, R.J., Hermann, J. & Richards, S., 2008, Submarine back-arc lava with arc signature; Fonulafei center, northeast Lau Basin, Tonga, Journal of Geophysical Research. v. 113, B08S07.

Kessel, R., Ulmer, P., Pettke, T., Schmidt, M.W. & Thompson, A.B., 2004, A novel approach to determine high-pressure high-temperature fluid and melt compositions using diamond-trap experiments. American Mineralogist v. 89, p. 1078-1086.

Mibe, K., Fujii, T. & Yasuda, A., 2002, Composition of aqueous fluid coexisting with mantle minerals at high pressure and its bearing on the differentiation of the Earth's mantle. Geochimica Cosmochimica Acta v. 66, p. 2273-2285.

Pearce, J.A., Stern, R.J., Bloomer, S.H. & Fryer, P., 2005, Geochemical mapping of the Mariana arc-basin system: Implications for the nature and distribution of subduction components. Geochemistry Geophysics Geosystems, v. 6, Q07006.

Pearce, N.J.G., Perkins, W.T., Westgate, J.A., Gorton, M.P., Jackson, S.E., Neal, C.B. & Chenery, S.P., 1997, A compilation of new and published major and trace element data for NIST SRM 610 and NIST SRM 612 glass reference materials. Geostandards News v. 21, p. 115-144.

Plank, T. & Langmuir, C.H., 1998 The chemical composition of subducting sediment and its consequences for the crust and mantle. Chemical Geology, v. 145, p. 325-394.

Schwab, B.E. & Johnston A.D., 2001, Melting systematics of modally variable, compositionally intermediate peridotites and the effects of mineral fertility. Journal of Petrology, v. 42, p. 1789-1811.

Rudnick, R.L. & Fountain, D.M., 1995, Nature and composition of the continental crust: A lower crustal perspective. Reviews in Geophysics. v. 33, no. 3, p. 267-309.

Stalder, R., Ulmer, P., Thompson, A.B. & Günther, D., 2001, High pressure fluids in the system $MgO-SiO_2-H_2O$ under upper mantle conditions. Contributions to Mineralogy and Petrology, v. 140, p. 607-618.

Tenthorey, E. & Hermann, J., 2004, Composition of fluids during serpentinite breakdown in subduction zones: evidence for limited boron mobility. Geology, v. 32, p. 865-868.

FIGURE CAPTIONS

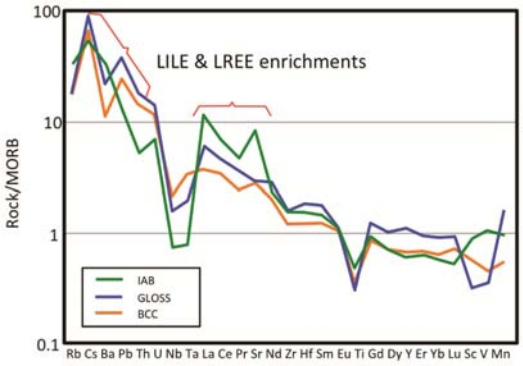

Figure DR1: Trace element pattern of subduction related rocks normalised on mid-ocean ridge basalts (MORB, Jenner and O'Neill, 2012). Island arc basalts (IAB, Pearce et al., 2005; Kelemen et al., 2004), Global subducted sediment (GLOSS, Plank and Langmuir, 1998) and bulk continental crust (BCC, Rudnick and Fountain, 1995) show enrichments in LILE and LREE and a negative anomaly in Nb and Ta. These features are generally labeled as the "slab component" of arc lavas and believed to be key characteristic of slab fluids.

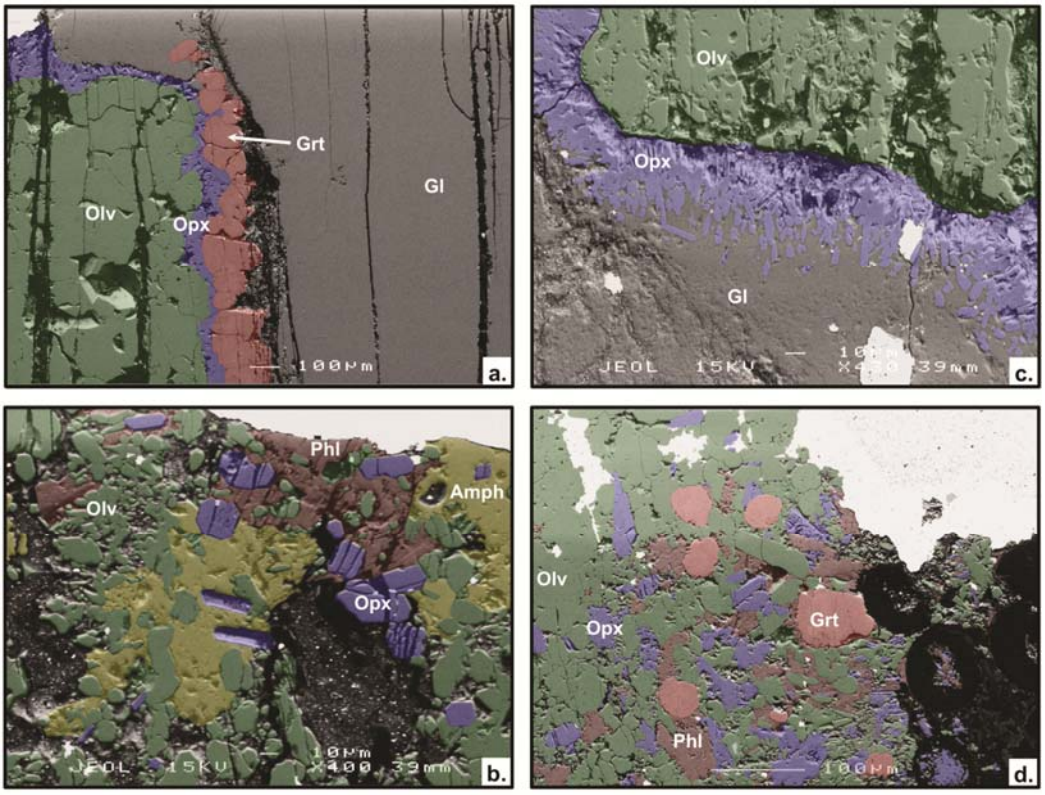

Figure DR2. BSE images of mixed and layered experiments with different starting materials. Bright white zones are parts of the gold capsules and uncoloured zones are aqueous fluid/melt-rich zones. Olivine (Olv), Orthopyroxene (Opx), Garnet (Grt), Phlogopite (Phl), Magnesiokatophorite (Amph) and Glass (Gl) are labelled. a. High-K layered experiment C2951 (1050 °C). The contact between recrystallised olivine and sediment melt features a continuous layer of garnet and orthopyroxene. b. Low-K layered experiment C3082 (800 °C). A continuous layer of orthopyroxene separates the recrystallised olivine and sediment melt. c. Low-K mixed experiment C3085 (950 °C). Rounded olivine and idiomorphic orthopyroxene are enclosed by large amphibole and phlogopite. Dark zones are holes produced during polishing of poorly cemented minerals and some voids occupied by aqueous fluids. d. High-K mixed experiment C2940 (1000 °C). Round garnet grains occur in a matrix of olivine and orthopyroxene with interstitial phlogopite. Pore space was likely occupied by fluid and dark round circles are polished carbon spheres.

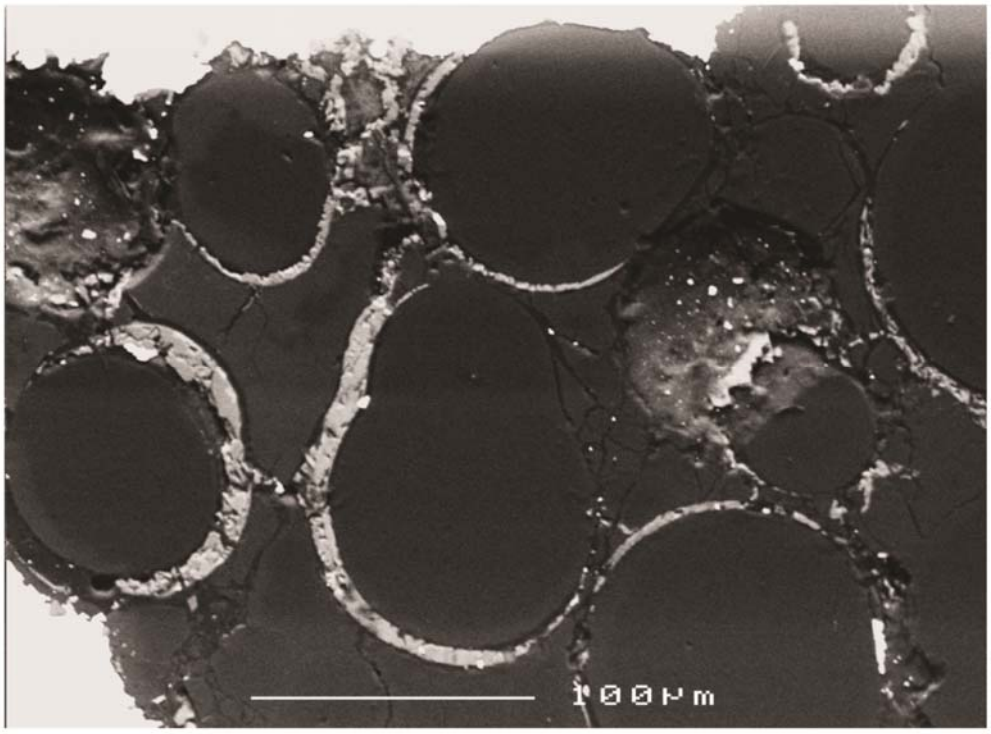

Figure DR3: Back-scattered electron image of carbon spheres (round dark) with trapped fluid quenched as glass (light grey) in C3083 (800 ºC) embedded in epoxy resin.

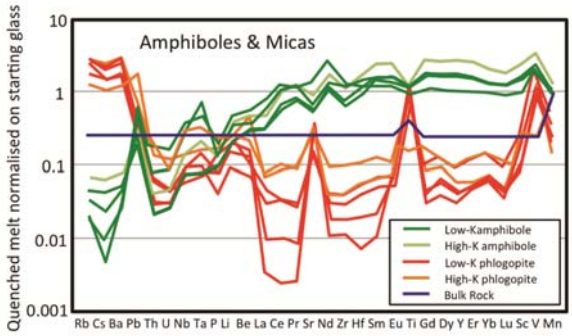

Figure DR4: Trace element pattern of amphiboles (green) and micas (orange-red) normalised on their respective starting glass. Amphiboles and micas have a complementary geochemical behaviour in this system. Micas are enriched in LILE and some transition metals, contains 0.4 to 1 wt.% TiO_2 but low Nb, Ta, Th and U compared to the starting material; amphiboles are poor in LILE but rich in REE and transition metals. HFSE are incompatible in both mineral phases.

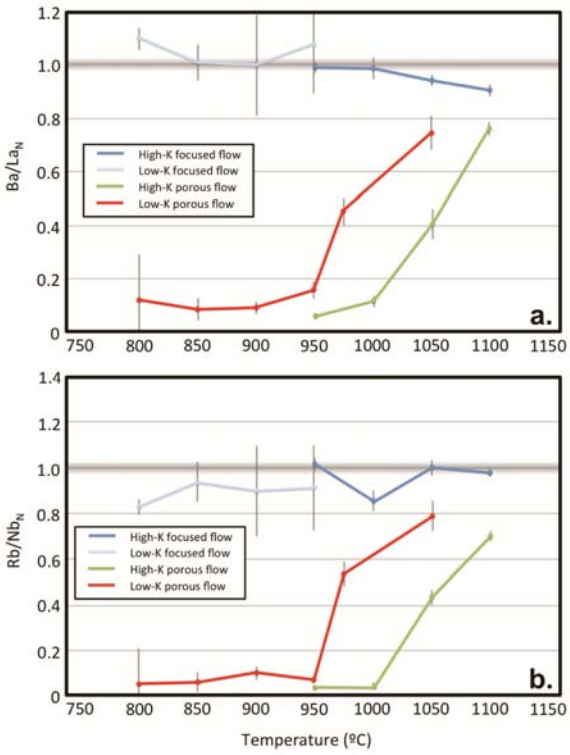

FigureDR 5: Variation of LILE, REE and HFSE with temperature in quenched fluids, normalised on respective starting material.

a. Ba/La_N is unmodified during focussed flow transfer while Ba/La is very low at sub-solidus conditions for porous flow due to the hosting potential of Ba in phlogopite. The change at 950 °C (low-K) and 1050 °C (high-K) is indicative of supra-solidus conditions when amphibole and mica are directly contributing to the Ba/La ratio of the hydrous melt.
b. Rb/Nb_N is unmodified during focussed flow transfer while Rb/Nb is very low at sub-solidus conditions for porous flow due to the hosting potential of Rb in phlogopite and the incompatibility of Nb in mica and amphibole.

TABLE DR1. EXPERIMENTAL CONDITIONS AND RUN PRODUCTS

Run no.	P (GPa)	T(ºC)	duration (h)	Assemblage	Products
C2933	3.5	950	168	High-K layered	Olv, Opx, Grt, *Mt, Co, Ky*
C2945	3.5	1000	168	High-K layered	Olv, Opx, Grt, Cpx, *Mt, Crd*
C2951	3.5	1050	168	High-K layered	Olv, Opx, Grt, *Mt*
D953	3.5	1100	168	High-K layered	Olv, Opx, Grt, Cpx, *Mt*
C3082	3.5	800	168	Low-K layered	Olv, Opx, Cpx, *Co, Mt*
C3076	3.5	850	168	Low-K layered	Olv, Opx, Cpx, *Co, Mt*
D965	3.5	900	168	Low-K layered	Olv, Opx, Cpx, *Mt*
D963	3.5	950	168	Low-K layered	Olv, Opx, *Mt*
C2910	3.5	950	168	High-K mixed	Olv, Opx, Grt, Phl, *Aq, Amph2, Crd*
C2940	3.5	1000	168	High-K mixed	Olv, Opx, Grt, Phl, *Aq, Amph2, Crd*
D891	3.5	1050	168	High-K mixed	Olv, Opx, Grt, Phl, *Mt, Amph2, Crd*
D979	3.5	1100	168	High-K mixed	Olv, Opx, Grt, Phl, *Mt, Amph2*
C3083	3.5	800	168	Low-K mixed	Olv, Opx, Phl, Amph1, *Aq*
D971	3.5	850	168	Low-K mixed	Olv, Opx, Phl, Amph1, *Aq*
D967	3.5	900	100	Low-K mixed	Olv, Opx, Phl, Amph1, *Aq*
D969	3.5	900	168	Low-K mixed	Olv, Opx, Phl, Amph1, *Aq, Crd*
C3085	3.5	950	168	Low-K mixed	Olv, Opx, Phl, Amph1, *Aq*
D1078	3.5	975	168	Low-K mixed	Olv, Opx, Phl, Amph1, *Mt* , *Amph2*
D1064	3.5	1000	168	Low-K mixed	Olv, Opx, Phl, Amph1, *Mt, Cpx, Amph2*
D1077	3.5	1050	168	Low-K mixed	Olv, Opx, Phl, *Mt* , *Amph2*

Olv : Olivine; Opx : Orthopyroxene; Grt : Garnet; Phl : Phlogopite; Amph1 : Magnesiokatophorite
Cpx : Omphacite; *Mt* : Melt (abundant glass); *Aq* : Aqueous Fluid (rare glass)
Co : Coesite, *Ky* : Kyanite, *Crd* : Corundum, *Amph2* : K-amphibole
Quenched phases are in italic

TABLE DR2. COMPOSITION OF PARAGENETIC AMPHIBOLES (MAGNESIOKATOPHORITE)

Exp	C3083	D971	D967	D969	C3085	D1064
P (Gpa)	3.5	3.5	3.5	3.5	3.5	3.5
T (ºC)	800	850	900	900	950	1000
n	6	3	6	14	4	12
SiO_2	50.7 (6)	51.0 (5)	51.4 (9)	50.9 (6)	49.2 (5)	49.7 (11)
TiO_2	0.53 (19)	0.76 (8)	0.50 (9)	0.62 (14)	0.46 (7)	0.51 (7)
Al_2O_3	8.5 (6)	9.9 (3)	9.2 (10)	9.2 (8)	10.1 (5)	9.9 (10)
FeO	4.4 (2)	3.9 (4)	4.5 (3)	4.3 (4)	3.7 (3)	4.2 (2)
MnO	0.06 (4)	0.09 (2)	n.d.	bdl	bdl	bdl
MgO	21.8 (7)	21.2 (6)	20.7 (7)	21.0 (7)	20.1 (2)	19.7 (4)
CaO	2.9 (8)	3.5 (4)	3.0 (3)	3.6 (6)	4.4 (0)	4.9 (6)
Na_2O	5.6 (5)	6.4 (4)	7.1 (3)	6.3 (3)	6.2 (3)	5.9 (2)
K_2O	0.26 (4)	0.84 (49)	0.45 (8)	0.37 (8)	0.55 (6)	0.64 (7)
Sum	94.8 (5)	97.7 (15)	96.9 (4)	96.3 (5)	94.6 (5)	95.6 (10)
Si	7.19 (6)	7.06 (7)	7.17 (8)	7.14 (10)	7.03 (6)	7.06 (13)
Ti	0.06 (2)	0.08 (1)	0.05 (1)	0.07 (1)	0.05 (1)	0.05 (1)
Al	1.43 (9)	1.62 (5)	1.52 (17)	1.52 (13)	1.69 (9)	1.66 (18)
Fe	0.52 (1)	0.46 (5)	0.53 (3)	0.51 (4)	0.44 (3)	0.50 (3)
Mn	0.01 (1)	0.01 (0)	-	-	-	-
Mg	4.61 (15)	4.38 (12)	4.31 (14)	4.39 (14)	4.27 (4)	4.18 (8)
Ca	0.44 (12)	0.52 (6)	0.45 (5)	0.54 (9)	0.67 (2)	0.75 (9)
Na	1.55 (14)	1.71 (11)	1.92 (6)	1.71 (10)	1.71 (9)	1.63 (7)
K	0.05 (1)	0.15 (9)	0.08 (1)	0.07 (2)	0.10 (2)	0.12 (1)
Σcat.	15.89	15.98	16.02	15.92	15.97	15.93
Mg#	0.899 (6)	0.906 (11)	0.891 (7)	0.896 (10)	0.907 (6)	0.894 (7)
K/(K+Na)	0.03 (1)	0.08 (4)	0.04 (6)	0.04 (1)	0.05 (1)	0.07 (1)
(00) are one standard deviation applied to the last decimal						
Li	13 (1)	5.1 (2)		9 (1)	5.4 (2)	n.d.
Be	26 (6)	24 (3)		17 (3)	12 (2)	13 (2)
B	20 (2)	23 (1)		19 (1)	19 (1)	n.d.
P	165 (47)	130 (97)		200 (43)	68 (14)	76 (12)
Sc	26 (4)	3.2 (1)		34 (6)	36 (3)	40 (7)
Ti	2453 (249)	5353 (65)		2787 (268)	3052 (382)	3307 (360)
V	70 (14)	39 (1)		72 (18)	76 (13)	80 (14)
Mn	692 (52)	162 (7)		751 (34)	676 (43)	741 (45)
Ni	1109 (229)	2182 (69)		958 (78)	1107 (114)	697 (281)
Rb	3 (5)	13 (4)		0.8 (3)	1.0 (3)	1.3 (2)
Sr	298 (60)	166 (3)		183 (18)	138 (36)	155 (13)
Y	19 (3)	0.38		29 (6)	30 (5)	33 (5)
Zr	165 (67)	10 (6)		159 (41)	80 (11)	98 (21)
Nb	21 (8)	21 (6)		11 (3)	5 (1)	6 (1)
Cs	5 (6)	7 (4)		0.42 (8)	0.22	0.3 (1)
Ba	49 (41)	102 (32)		16 (3)	18 (9)	19 (2)
La	26 (7)	3 (3)		21 (4)	10 (3)	11 (1)
Ce	68 (15)	3 (3)		60 (10)	30 (8)	35 (2)
Pr	39 (9)	1 (1)		37 (9)	24 (7)	27 (2)
Nd	45 (9)	n.d.		50 (12)	36 (10)	41 (3)
Sm	41 (8)	2.3 (2)		54 (14)	49 (11)	55 (5)
Eu	41 (7)	1.7 (3)		56 (11)	48 (8)	57 (6)
Gd	38 (6)	n.d.		58 (12)	60 (13)	65 (9)
Dy	37 (7)	n.d.		58 (14)	60 (11)	67 (10)
Er	18 (4)	n.d.		26 (6)	27 (4)	31 (5)
Yb	18 (3)	n.d.		24 (5)	24 (3)	27 (4)
Lu	17 (2)	1		22 (4)	20 (3)	23 (3)
Hf	25 (10)	2 (1)		32 (9)	21 (4)	25 (7)
Ta	12 (5)	23 (24)		7 (2)	4 (1)	3 (1)
Pb	43 (31)	1.4 (5)		12 (8)	7 (4)	4 (6)
Th	2 (1)	1.8 (1)		1 (1)	0.6 (2)	0.5 (1)
U	2 (1)	2.4 (4)		2 (1)	0.6 (2)	0.6 (2)

TABLE DR4. COMPOSITION OF MICAS (PHLOGOPITE)

Exp	C3083	D971	D967	D969	C3085	D1078	D1064	D1077	C2910	C2940	D891	D979
P (Gpa)	3.5	3.5	3.5	3.5	3.5	3.5	3.5	3.5	3.5	3.5	3.5	3.5
T (ºC)	800	850	900	900	950	975	1000	1050	950	1000	1050	1100
n	5	7	4	14	6	5	7	5	6	7	5	9
SiO_2	42.5 (16)	41.8 (5)	41.4 (4)	41.5 (7)	40.8 (7)	40.9 (5)	40.7 (3)	43.2 (4)	40.8 (8)	39.1 (6)	40.9 (5)	41.5 (11)
TiO_2	0.38 (7)	0.39 (8)	0.52 (8)	0.50 (13)	0.49 (6)	0.67 (8)	0.49 (11)	1.10 (34)	0.57 (22)	0.46 (9)	0.45 (10)	0.44 (11)
Al_2O_3	12.3 (12)	13.1 (5)	13.2 (8)	13.4 (5)	13.4 (5)	14.0 (2)	13.7 (4)	11.4 (6)	13.5 (2)	13.4 (4)	14.5 (3)	14.3 (5)
FeO	3.7 (32)	3.5 (10)	3.7 (14)	3.5 (34)	3.4 (13)	2.5 (21)	3.9 (16)	3.5 (47)	3.4 (3)	3.8 (3)	3.6 (3)	3.7 (3)
MnO	bdl	bdl	n.d.	bdl	bdl	bdl	bdl	0.16 (8)	0.22 (17)	bdl	bdl	bdl
MgO	24.6 (5)	25.0 (6)	24.5 (3)	24.9 (5)	24.5 (3)	24.6 (4)	23.8 (3)	23.4 (8)	24.7 (2)	23.6 (6)	24.9 (3)	24.5 (7)
CaO	bdl	bdl	0.09 (7)	bdl	bdl	bdl	bdl	bdl	bdl	bdl	bdl	bdl
Na_2O	1.9 (1)	1.9 (2)	1.4 (6)	2.0 (3)	1.7 (2)	1.3 (1)	1.6 (1)	1.4 (3)	1.2 (2)	0.9 (2)	0.8 (2)	9.7 (10)
K_2O	6.2 (1)	6.8 (3)	8.3 (7)	7.2 (4)	7.5 (5)	8.2 (2)	7.8 (1)	6.9 (9)	8.8 (2)	9.0 (2)	9.6 (2)	0.7 (6)
Sum	91.7 (12)	92.4 (9)	93.2 (9)	92.9 (15)	91.9 (6)	92.2 (9)	92.1 (14)	91.1 (7)	93.2 (12)	90.3 (17)	94.8 (7)	94.8 (26)
Si	3.05 (9)	2.98 (4)	2.97 (5)	2.97 (2)	2.94 (4)	2.97 (2)	2.95 (2)	3.13 (3)	2.93 (2)	2.89 (1)	2.88 (1)	2.93 (3)
Ti	0.02 (0)	0.02 (0)	0.03 (0)	0.03 (1)	0.03 (0)	0.03 (1)	0.03 (1)	0.06 (2)	0.03 (1)	0.03 (0)	0.03 (1)	0.02 (1)
Al	1.04 (11)	1.11 (4)	1.11 (4)	1.13 (6)	1.15 (5)	1.19 (2)	1.17 (2)	0.98 (6)	1.15 (1)	1.17 (2)	1.20 (3)	1.19 (2)
Fe	0.22 (2)	0.21 (1)	0.22 (1)	0.21 (2)	0.21 (1)	0.15 (1)	0.24 (1)	0.21 (4)	0.20 (2)	0.21 (2)	0.20 (1)	0.22 (1)
Mn	-	-	-	-	-	-	-	tr.	tr.	tr.	tr.	tr.
Mg	2.63 (8)	2.66 (5)	2.62 (2)	2.65 (3)	2.64 (3)	2.65 (2)	2.57 (1)	2.52 (8)	2.65 (2)	2.61 (3)	2.61 (3)	2.58 (3)
Ca	-	-	tr.	-	-	-	-	-	tr.	tr.	tr.	tr.
Na	0.27 (2)	0.26 (2)	0.20 (8)	0.27 (4)	0.25 (3)	0.18 (1)	0.23 (1)	0.19 (6)	0.16 (2)	0.13 (2)	0.10 (3)	0.88 (7)
K	0.57 (1)	0.62 (2)	0.76 (7)	0.66 (4)	0.70 (5)	0.76 (2)	0.72 (1)	0.64 (8)	0.81 (3)	0.85 (2)	0.88 (2)	0.10 (8)
Σcat.	7.80	7.86	7.91	7.91	7.91	7.94	7.90	7.73	7.93	7.88	7.89	7.92
Mg#	0.922 (4)	0.928 (2)	0.923 (3)	0.927 (6)	0.926 (3)	0.945 (4)	0.916 (3)	0.923 (6)	0.929 (5)	0.924 (5)	0.930 (5)	0.921 (4)
K/(K+Na)	0.68 (1)	0.70 (2)	0.80 (8)	0.70 (4)	0.74 (3)	0.80 (1)	0.76 (1)	0.77 (6)	0.83 (2)	0.87 (2)	0.89 (3)	0.90 (8)

(00) are one standard deviation applied to the last decimal

Li	6 (1)	7 (1)		8 (1)	5.8 (4)						8	
Be	7 (3)	8 (1)		7 (2)	5 (1)	3 (1)	6 (1)	7	14 (2)	6.5 (4)	5 (2)	
B	16 (1)	16 (1)		17 (1)	18 (1)				11.8 (5)	11 (1)	17	
P	136	107		226	128	39	74	86		102 (55)	278 (40)	
Sc	5 (1)	5 (2)		5 (1)	3 (1)	5 (1)	2.7 (5)	2	2.9 (2)	4 (1)	5 (40)	
Ti	631 (247)	1015 (118)		961 (147)	1846 (178)	3375 (873)	2817 (242)	2631	4045 (15)	1412 (795)		
V	13 (4)	16 (5)		18 (2)	27 (8)	40 (7)	31 (7)	27	42 (3)	29 (9)	6 (6)	
Mn	682 (119)	614 (29)		554 (48)	297 (58)	251 (113)	169 (16)	142	136 (1)	464 (203)	948 (856)	
Ni	1593 (277)	1572 (411)		710 (151)	1324 (398)	738 (375)	946 (636)	1015	1473 (360)	1379 (336)	949 (395)	
Cu						1	1	1	1	3 (3)	9 (1)	
Zn									43 (10)	37 (4)	54 (4)	
Rb	23 (18)	40 (3)		35 (7)	91 (19)	118 (27)	127 (8)	130	87 (6)	38 (27)	60 (11)	
Sr	34 (16)	63 (13)		64 (14)	65 (5)	43 (7)	85 (10)	99	131 (19)	51 (22)	87 (25)	
Y	1.6 (5)	2 (1)		2 (1)	0.5 (3)	1 (1)	0.2 (1)		13	1 (1)	1 (32)	
Zr	11 (3)	26 (34)		16 (11)	4 (3)	5 (5)	2 (1)	1	2.7 (2)	8 (6)	20 (19)	
Nb	8 (2)	4.7 (2)		9 (4)	3 (1)	5 (1)	4.5 (3)	4	11.2 (4)	5.3 (1)	8 (2)	
Cs	19 (13)	25 (4)		29 (7)	69 (14)	73 (15)	98 (3)	106	75 (5)	33 (25)	4 (8)	
Ba	215 (139)	317 (46)		423 (98)	884 (118)	958 (229)	1347 (83)	1476	1029 (91)	407 (292)	42 (113)	
La	6 (1)	4 (1)		6 (3)	2 (1)	1 (1)	0.3 (2)	0.1	2	2 (2)	6.4 (3)	
Ce	9 (2)	7 (3)		10 (5)	2 (1)	2 (2)	0.5 (4)	0.1		3 (4)	11 (1)	
Pr	3 (1)	3 (2)		4 (2)	1 (1)	1 (1)	0.3 (3)	0.1		2 (2)	5.3 (1)	
Nd	3 (1)	3 (2)		4 (3)		1 (1)				2 (2)	6 (1)	
Sm	3 (2)	3 (2)		3 (2)		2 (2)				3	5	
Eu	3 (1)	3 (2)		3 (2)	2 (1)	2 (1)	2.3 (3)	2	1.3 (1)	3 (2)	5 (6)	
Gd	4 (1)	5 (1)		2 (3)	1	2 (1)				2 (2)	4	
Dy	3 (1)	4 (3)		3 (2)	1	2 (1)				2	3	
Er	1.6 (4)	2 (1)		2 (1)		1 (1)				0.7 (5)	1	
Yb	1.8 (3)	2 (1)		2 (1)		2 (1)				1	1	
Lu	1.7 (3)	2 (1)		2 (1)	0.7 (3)	1 (1)				0.5 (4)	1 (63)	
Hf	1.7 (5)	3 (3)		2 (1)	1	1 (1)	0.4 (1)	0.2		2 (1)	3 (3)	
Ta	3 (1)	2.5 (1)		4 (2)	1.7 (4)	2 (1)	2.0 (4)	2	5.3 (3)	2.6 (3)	3 (1)	
Pb	6 (7)	4 (3)		2.1 (5)	4 (3)	4 (3)	4 (4)	4	8 (6)	20 (7)	21 (3)	
Th	5 (1)	6 (1)		4 (1)	1.2 (4)	1 (1)	0.5 (2)	0.4	2 (1)	1 (1)	3	
U	7 (3)	6 (1)		5 (2)	0.9 (2)	1 (1)	0.6 (2)	1	1.2 (4)	2 (1)	5	

TABLE DR5. MAJOR AND TRACE ELEMENT COMPOSITION OF EXPERIMENTALLY PRODUCED GLASSES

	Starting Materials														
Exp	D897	C2964/D1080	D1078	D1064	D1077	D891	D979	C2933	C2945	C2951	D953	C3082	C3076	D965	D963
			Porous	Porous	Porous	Porous	Porous	Focused	Focused	Focused	Focused	Focused	Focused	Focused	Focused
	High-K	Low-K	Low-K	Low-K	Low-K	High-K	High-K	High-K	High-K	High-K	High-K	Low-K	Low-K	Low-K	Low-K
P (Gpa)	3.5	1.5	3.5	3.5	3.5	3.5	3.5	3.5	3.5	3.5	3.5	3.5	3.5	3.5	3.5
T (ºC)	950	800	975	1000	1050	1050	1100	950	1000	1050	1100	800	850	900	950
SiO_2	70.3 (9)	64 (2)	47 (1)	37 (5)	40 (0)	47 (6)	55 (8)	69 (1)	69 (1)	68 (0)	64 (1)	64 (1)	66 (0)	66 (1)	62 (1)
TiO_2	0.39 (1)	0.3 (1)	0.47 (8)	0.42 (20)	0.20 (11)	0.79 (61)	0.54 (40)	0.49 (10)	0.41 (13)	0.47 (17)	0.38 (10)	0.34 (17)	0.33 (11)	0.28 (12)	0.27 (9)
Al_2O_3	13.8 (2)	10.8 (4)	13.1 (3)	10.5 (17)	11.7 (1)	13.0 (21)	13.6 (21)	13.8 (4)	13.4 (3)	12.8 (2)	13.8 (2)	10.7 (6)	11.0 (1)	11.0 (2)	10.9 (2)
FeO	0.82 (5)	0.8 (3)	2.0 (4)	3.0 (13)	3.9 (1)	4.4 (7)	4.8 (13)	0.5 (2)	0.4 (2)	1.1 (3)	2.6 (1)	0.3 (3)	0.5 (2)	0.7 (1)	0.7 (3)
MnO	0.07 (2)	0.1 (1)	0.03 (3)	0.03 (4)	0.18 (1)	0.11 (14)	0.11 (30)	0.02 (11)	0.05 (9)	0.05 (11)	0.06 (13)	0.04 (12)	0.04 (11)	0.02 (9)	0.02 (6)
MgO	0.39 (2)	0.4 (1)	4.1 (3)	4.3 (22)	9.3 (2)	9.2 (16)	7.3 (12)	0.5 (1)	0.4 (9)	2.9 (16)	1.7 (8)	0.2 (26)	0.4 (19)	0.8 (9)	0.9 (35)
CaO	0.81 (1)	1.2 (8)	1.2 (2)	0.6 (2)	1.8	1.7 (1)	1.1 (4)	0.7 (1)	0.2 (1)	1.1 (2)	0.9 (1)	0.2 (3)	0.2 (1)	0.3 (1)	0.8 (4)
Na_2O	2.1 (1)	4.8 (3)	7.6 (15)	9.4 (22)	5.0 (1)	6.5 (4)	6.9 (39)	3.1 (7)	4.6 (9)	2.9 (2)	4.5 (7)	3.5 (5)	4.2 (3)	4.7 (5)	5.7 (2)
K_2O	6.0 (1)	2.9 (2)	2.0 (1)	2.3 (22)	3.6 (0)	3.5 (7)	2.8 (3)	5.5 (4)	5.1 (2)	4.8 (1)	6.5 (1)	4.5 (5)	3.7 (2)	3.0 (2)	2.7 (2)
H_2O meas.	94.6 (8)	85 (2)	22 (1)	33 (2)	24 (4)	14 (4)	8 (2)	6 (1)	6 (1)	6 (0)	6 (1)	16 (1)	14 (1)	13 (1)	16 (1)
(00) are one standard deviation applied to the last decimal															
H_2O measured by difference															
Li	29	19	56 (3)	82 (8)	43 (2)	41 (4)	22 (1)	29 (1)	19 (1)	24 (1)	23 (0)	21 (5)	22 (4)	18 (0)	17 (1)
Be	48	31	n.d.	n.d.	n.d.	142 (15)	106 (3)	53 (1)	46 (2)	43 (1)	45 (1)	38 (7)	37 (7)	38 (1)	33 (0)
B	70	46	n.d.	77 (7)	n.d.	111 (11)	82 (2)	33 (0)	35 (1)	39 (0)	26 (0)	26 (2)	28 (3)	23 (1)	23 (0)
P	1002	653	1509 (94)	1013 (97)	997 (51)	1705 (174)	1018 (28)	1015 (13)	1098 (69)	949 (9)	939 (23)	721 (131)	710 (151)	771 (11)	706 (9)
Sc	27	17	15 (1)	12 (1)	19 (1)	22 (2)	19 (1)	15 (1)	11 (2)	13 (0)	13 (1)	24 (11)	25 (17)	7 (0)	13 (0)
Ti	2835	1847	2829 (176)	2501 (239)	2947 (149)	4420 (451)	3006 (81)	2944 (28)	2438 (181)	2804 (28)	2301 (23)	2031 (273)	2004 (337)	1677 (19)	1608 (12)
V	36	24	9 (1)	8 (1)	18 (1)	29 (3)	12 (0)	28 (1)	9 (4)	38 (0)	30 (4)	75 (47)	59 (45)	4 (0)	22 (1)
Mn	732	1163	234 (15)	236 (23)	514 (26)	797 (81)	810 (22)	162 (2)	388 (32)	386 (2)	435 (4)	312 (167)	320 (206)	139 (1)	163 (3)
Ni			10 (1)	31 (3)	19 (1)	23 (2)	20 (1)	0 (0)	0	2 (0)	1 (1)	9 (5)	12 (12)	1 (1)	1 (0)
Cu			n.d.	25 (2)	n.d.	47 (5)	6 (0)	2 (0)	3 (0)	2 (0)	5 (0)	5 (1)	5 (1)	4 (0)	4 (0)
Zn			n.d.	14 (1)	n.d.	33 (3)	23 (1)	7 (0)	7 (0)	18 (0)	20 (0)	42 (7)	34 (8)	14 (0)	15 (0)
Rb	50	33	30 (2)	9 (1)	34 (2)	61 (6)	61 (2)	63 (1)	51 (1)	48 (0)	51 (1)	39 (11)	40 (11)	43 (1)	37 (1)
Sr	288	187	333 (21)	444 (42)	258 (13)	1317 (134)	470 (13)	331 (4)	320 (14)	283 (3)	255 (4)	228 (44)	215 (37)	219 (4)	208 (51)
Y	19	13	26 (2)	31 (3)	22 (1)	32 (3)	62 (2)	9 (1)	15 (1)	18 (0)	14 (0)	15 (2)	15 (1)	12 (0)	13 (1)
Zr	140	91	279 (17)	421 (40)	193 (10)	514 (52)	370 (10)	148 (3)	150 (9)	136 (2)	138 (4)	134 (18)	126 (17)	125 (5)	109 (1)
Nb	61	40	68 (4)	115 (11)	53 (3)	170 (17)	108 (3)	62 (1)	64 (4)	56 (0)	62 (1)	55 (9)	52 (11)	55 (2)	46 (1)
Cs	50	32	20 (1)	22 (2)	39 (2)	30 (3)	53 (1)	51 (1)	44 (1)	46 (0)	49 (1)	37 (8)	39 (12)	41 (1)	34 (1)
Ba	546	355	384 (24)	176 (17)	518 (26)	886 (90)	981 (27)	643 (3)	640 (26)	551 (9)	494 (6)	463 (107)	442 (93)	448 (9)	438 (153)
La	36	23	55 (3)	100 (10)	46 (2)	142 (15)	85 (2)	43 (1)	43 (1)	38 (1)	36 (1)	28 (5)	29 (5)	29 (1)	27 (1)
Ce	56	37	71 (4)	120 (11)	59 (3)	211 (22)	99 (3)	72 (1)	71 (2)	62 (1)	60 (1)	46 (7)	48 (8)	50 (1)	45 (2)
Pr	34	22	41 (3)	66 (6)	34 (2)	121 (12)	64 (2)	39 (1)	39 (1)	35 (0)	33 (1)	26 (3)	26 (4)	26 (1)	25 (1)
Nd	37	24	50 (3)	77 (7)	41 (2)	140 (14)	82 (2)	43 (1)	42 (1)	39 (1)	37 (1)	28 (3)	29 (3)	28 (1)	26 (1)
Sm	36	23	47 (3)	63 (6)	37 (2)	122 (12)	76 (2)	36 (1)	36 (1)	36 (1)	33 (1)	27 (1)	28 (1)	25 (1)	24 (1)
Eu	37	24	42 (3)	55 (5)	34 (2)	107 (11)	64 (2)	37 (1)	37 (1)	35 (1)	31 (1)	28 (1)	28 (1)	24 (1)	24 (1)
Gd	37	24	52 (3)	64 (6)	41 (2)	104 (11)	79 (2)	29 (1)	33 (1)	33 (1)	30 (1)	28 (2)	28 (2)	23 (0)	23 (1)
Dy	39	25	51 (3)	58 (6)	41 (2)	72 (7)	68 (2)	20 (1)	30 (1)	28 (1)	26 (1)	29 (4)	30 (3)	23 (0)	24 (1)
Er	19	13	25 (2)	28 (3)	21 (1)	25 (3)	30 (1)	8 (1)	15 (1)	11 (0)	10 (0)	15 (2)	15 (2)	11 (0)	11 (1)
Yb	20	13	24 (1)	27 (3)	21 (1)	21 (2)	25 (1)	7 (1)	15 (0)	8 (0)	9 (0)	15 (2)	15 (2)	12 (0)	12 (0)
Lu	19	13	23 (1)	26 (2)	21 (1)	19 (2)	23 (1)	7 (1)	15 (0)	7 (0)	8 (0)	15 (2)	14 (1)	11 (0)	11 (0)
Hf	23	15	47 (3)	64 (6)	32 (2)	80 (8)	57 (2)	23 (0)	23 (1)	22 (0)	20 (1)	20 (2)	20 (2)	18 (1)	16 (0)
Ta	26	17	39 (2)	63 (6)	28 (1)	82 (8)	57 (2)	26 (1)	28 (2)	24 (0)	25 (1)	23 (4)	22 (4)	22 (1)	19 (0)
Pb	19	12	6 (0)	12 (1)	31 (2)	186 (19)	21 (1)	12 (0)	6 (1)	23 (0)	22 (1)	4 (1)	3 (1)	2 (0)	3 (1)
Th	18	12	33 (2)	59 (6)	27 (1)	74 (8)	48 (1)	20 (0)	20 (2)	18 (1)	17 (1)	16 (3)	16 (3)	16 (1)	14 (0)
U	21	14	21 (1)	38 (4)	18 (1)	75 (8)	33 (1)	24 (0)	24 (2)	21 (0)	21 (1)	20 (3)	19 (4)	20 (1)	17 (1)

TABLE DR6. MAJOR AND TRACE ELEMENT COMPOSITION CALCULATED FROM QUENCHED PRODUCTS

	Starting Materials																
Exp	D897	C2964/D1080	C3083	C3083 - 10% Amph	D971	D971 - 10% Amph	D969	D969 - 10% Amph	C3085	C3085 - 10% Amph	D1078	D1064	D1077	C2910	C2940	D891	D979
			Porous		Porous		Porous		Porous		Porous	Porous	Porous	Porous	Porous	Porous	Porous
	High-K	Low-K	Low-K		Low-K		Low-K		Low-K		Low-K	Low-K	Low-K	High-K	High-K	High-K	High-K
P (Gpa)	3.5	1.5	3.5		3.5		3.5		3.5		3.5	3.5	3.5	3.5	3.5	3.5	3.5
T (ºC)	950	800	800		850		900		950		975	1000	1050	950	1000	1050	1100
SiO_2	70.3 (9)	64 (2)	15 (2)	11 (2)	16 (1)	12 (1)	15 (1)	11 (1)	19 (1)	16 (1)	43 (2)	34 (2)	38 (2)	24 (2)	27 (3)	46 (5)	53 (1)
TiO_2	0.39 (1)	0.3 (1)	0.15 (2)	0.02 (2)	0.19 (2)	0.08 (2)	0.16 (1)	0.10 (1)	0.30 (2)	0.25 (2)	0.44 (2)	0.39 (3)	0.19 (2)	0.80 (5)	0.81 (8)	0.77 (8)	0.52 (1)
Al_2O_3	13.8 (2)	10.8 (4)	1.9 (2)	1.2 (2)	2.3 (2)	1.5 (2)	2.3 (1)	1.5 (1)	3.1 (2)	2.3 (2)	12.2 (6)	9.8 (6)	11.0 (5)	8.2 (5)	9.9 (9)	12.6 (13)	13.1 (4)
FeO	0.82 (5)	0.8 (3)	1.0 (1)	0.6 (1)	1.0 (1)	0.7 (1)	1.0 (1)	0.6 (1)	1.3 (1)	1.0 (1)	1.8 (1)	2.8 (2)	3.6 (4)	0.6 (0)	2.5 (2)	4.2 (4)	4.6 (1)
MnO	0.07 (2)	0.1 (1)	0.01 (0)	bdl	0.01 (0)	bdl	0.01 (0)	bdl	0.03 (0)	0.01 (0)	0.03 (1)	0.03 (1)	0.17 (5)	0.05 (0)	0.08 (1)	0.10 (1)	0.11 (0)
MgO	0.39 (2)	0.4 (1)	5.7 (6)	3.9 (6)	6.3 (6)	4.7 (6)	4.0 (24)	2.1 (24)	7.7 (4)	6.4 (4)	3.8 (2)	4.1 (3)	8.8 (5)	2.1 (1)	5.0 (5)	8.9 (9)	7.1 (2)
CaO	0.81 (1)	1.2 (8)	1.8 (2)	1.7 (2)	1.2 (1)	1.0 (1)	1.0 (6)	0.7 (6)	1.9 (1)	1.6 (1)	1.1 (1)	0.6 (1)	1.7 (7)	2.9 (2)	2.6 (3)	1.6 (2)	1.1 (0)
Na_2O	2.1 (1)	4.8 (3)	1.8 (2)	1.4 (2)	1.9 (2)	1.5 (2)	1.8 (1)	1.3 (1)	2.3 (1)	1.9 (1)	7.0 (3)	8.8 (5)	4.7 (10)	9.1 (6)	11.1 (11)	6.3 (6)	6.7 (2)
K_2O	6.0 (1)	2.9 (2)	0.4 (1)	0.4 (1)	0.38 (3)	0.33 (3)	0.32 (3)	0.32 (3)	0.3 (2)	0.3 (2)	1.8 (1)	2.1 (1)	3.4 (3)	1.8 (1)	2.2 (2)	3.4 (3)	2.7 (1)
H_2O calc.	94.6 (8)	85 (2)	72 (8)	80 (8)	71 (9)	78 (9)	75 (4)	83 (4)	64 (2)	70 (2)	28 (4)	37 (1)	24 (4)	51 (3)	39 (4)	16 (2)	11 (0)
(00) are one standard deviation applied to the last decimal																	
Li	29	19	23 (3)	24 (9)	18 (1)	20 (3)	14 (4)	14 (5)	13 (2)	14 (3)	52 (3)	77 (7)	41 (2)	30 (9)	31 (7)	41 (4)	22 (1)
Be	48	31	129 (30)	140 (63)	118 (2)	129 (14)	77 (7)	84 (16)	95 (13)	104 (22)	n.d.	n.d.	n.d.	255 (85)	247 (43)	142 (15)	106 (3)
B	70	46	356 (96)	392 (188)	144 (22)	158 (36)	72 (25)	78 (34)	62 (6)	67 (12)	n.d.	72 (7)	n.d.	248 (67)	137 (12)	111 (11)	82 (2)
P	1002	653	6457 (1140)	7127 (2800)	3680 (410)	4098 (768)	1295 (151)	1423 (304)	1753 (384)	1951 (555)	1399 (87)	949 (91)	941 (48)	5625 (1800)	3400 (323)	1705 (174)	1018 (28)
Sc	27	17	3 (1)	1 (2)	2 (0)	2 (0)	3 (1)		7 (2)	4 (3)	14 (1)	11 (1)	18 (1)	10 (3)	15 (2)	22 (2)	19 (1)
Ti	2835	1847	885 (345)	708 (572)	1146 (334)	798 (445)	977 (93)	782 (208)	1805 (149)	1678 (325)	2623 (163)	2344 (224)	2782 (141)	4576 (1840)	4706 (526)	4420 (451)	3006 (81)
V	36	24	5 (3)	(5)	4 (1)	1 (2)	5 (1)		6 (1)		8 (0)	8 (1)	17 (1)	21 (4)	38 (6)	29 (3)	12 (0)
Mn	732	1163	93 (32)	26 (56)	70 (7)	45 (14)	100 (25)	29 (37)	236 (14)	189 (37)	217 (13)	221 (21)	485 (25)	360 (116)	603 (101)	797 (81)	810 (22)
Ni			42 (45)	(56)	20 (12)		28 (17)		46 (27)		9 (1)	29 (3)	18 (1)	61 (42)	62 (24)	23 (2)	20 (1)
Cu			13 (1)	(4)	47 (14)		n.d.	n.d.	n.d.	n.d.	n.d.	23 (2)	n.d.	10 (26)	55 (67)	47 (5)	6 (0)
Zn			7 (2)	(4)	12 (5)		n.d.	n.d.	n.d.	n.d.	n.d.	13 (1)	n.d.	23 (29)	37 (28)	33 (3)	23 (1)
Rb	50	33	13 (3)	14 (6)	10 (2)	8 (3)	8 (3)	9 (4)	7 (1)	8 (2)	27 (2)	8 (1)	32 (2)	17 (15)	11 (7)	61 (6)	61 (2)
Sr	288	187	391 (62)	400 (163)	602 (264)	657 (323)	282 (22)	294 (55)	427 (60)	462 (102)	309 (19)	416 (40)	244 (12)	1973 (694)	1630 (314)	1317 (134)	470 (13)
Y	19	13	5 (1)	4 (2)	5 (0)	6 (1)	8 (1)	5 (2)	25 (2)	25 (5)	24 (2)	29 (3)	21 (1)	16 (5)	29 (5)	32 (3)	62 (2)
Zr	140	91	175 (37)	176 (82)	165 (42)	184 (58)	186 (27)	190 (49)	357 (39)	390 (73)	258 (16)	394 (38)	183 (9)	899 (280)	1095 (193)	514 (52)	370 (10)
Nb	61	40	257 (61)	282 (127)	193 (12)	214 (31)	94 (9)	103 (20)	116 (16)	129 (27)	63 (4)	107 (10)	50 (3)	577 (218)	388 (68)	170 (17)	108 (3)
Cs	50	32	60 (17)	65 (32)	41 (9)	45 (13)	34 (19)	38 (23)	19 (4)	21 (6)	19 (1)	20 (2)	37 (2)	46 (26)	32 (10)	30 (3)	53 (1)
Ba	546	355	144 (8)	154 (45)	87 (16)	80 (24)	90 (28)	98 (39)	226 (44)	251 (66)	356 (22)	165 (16)	490 (25)	361 (358)	532 (72)	886 (90)	981 (27)
La	36	23	73 (20)	78 (39)	71 (10)	79 (17)	67 (9)	72 (17)	97 (11)	107 (20)	51 (3)	94 (9)	43 (2)	443 (177)	311 (60)	142 (15)	85 (2)
Ce	56	37	65 (15)	64 (32)	62 (6)	68 (12)	68 (10)	70 (18)	113 (13)	122 (24)	66 (4)	112 (11)	56 (3)	631 (255)	448 (84)	211 (22)	99 (3)
Pr	34	22	23 (4)	21 (10)	26 (2)	29 (5)	29 (4)	28 (7)	60 (6)	65 (12)	38 (2)	62 (6)	32 (2)	348 (146)	254 (49)	121 (12)	64 (2)
Nd	37	24	23 (3)	20 (9)	23 (2)	25 (4)	29 (3)	27 (6)	68 (7)	72 (13)	47 (3)	73 (7)	39 (2)	360 (137)	283 (55)	140 (14)	82 (2)
Sm	36	23	12 (1)	8 (4)	15 (2)	17 (3)	18 (2)	14 (4)	53 (4)	54 (9)	44 (3)	59 (6)	35 (2)	200 (76)	223 (45)	122 (12)	76 (2)
Eu	37	24	11 (1)	8 (4)	12 (1)	13 (2)	17 (1)	13 (3)	44 (4)	44 (8)	38 (2)	52 (5)	32 (2)	154 (61)	178 (35)	107 (11)	64 (2)
Gd	37	24	9 (1)	5 (3)	10 (1)	11 (2)	15 (2)	10 (4)	48 (4)	47 (9)	48 (3)	59 (6)	39 (2)	123 (45)	166 (31)	104 (11)	79 (2)
Dy	39	25	8 (2)	4 (4)	8 (0)	9 (1)	13 (2)	8 (4)	43 (3)	41 (7)	47 (3)	54 (5)	39 (2)	53 (20)	84 (17)	72 (7)	68 (2)
Er	19	13	4 (1)	2 (2)	4 (0)	4 (1)	6 (1)	4 (2)	21 (2)	20 (4)	23 (1)	26 (2)	20 (1)	11 (5)	20 (3)	25 (3)	30 (1)
Yb	20	13	4 (1)	3 (2)	5 (1)	5 (1)	7 (1)	5 (2)	22 (2)	21 (4)	22 (1)	25 (2)	20 (1)	6 (2)	13 (2)	21 (2)	25 (1)
Lu	19	13	4 (0)	3 (1)	5 (0)	5 (1)	7 (1)	5 (2)	21 (2)	21 (4)	21 (1)	24 (2)	20 (1)	4 (1)	10 (2)	19 (2)	23 (1)
Hf	23	15	16 (2)	15 (6)	18 (1)	19 (3)	21 (3)	20 (6)	48 (4)	52 (9)	44 (3)	60 (6)	30 (2)	172 (57)	177 (31)	80 (8)	57 (2)
Ta	26	17	77 (18)	84 (38)	76 (6)	83 (13)	42 (6)	46 (11)	63 (8)	69 (14)	37 (2)	59 (6)	26 (1)	234 (90)	193 (32)	82 (8)	57 (2)
Pb	19	12	18 (2)	15 (7)	49 (37)	54 (42)	9 (2)	8 (3)	16 (2)	17 (4)	6 (0)	11 (1)	29 (1)	103 (178)	169 (64)	186 (19)	21 (1)
Th	18	12	29 (8)	32 (15)	22 (3)	25 (5)	31 (6)	35 (9)	59 (8)	66 (13)	31 (2)	55 (5)	25 (1)	209 (83)	172 (28)	74 (8)	48 (1)
U	21	14	40 (12)	44 (22)	28 (2)	31 (5)	25 (5)	28 (8)	38 (5)	43 (9)	20 (1)	36 (3)	17 (1)	188 (72)	159 (28)	75 (8)	33 (1)